

Active pump-seed-pulse synchronization for OPCPA with sub-2-fs residual timing jitter

Stephan Prinz,^{1,2,*} Matthias Häfner,¹ Marcel Schultze,¹ Catherine Y. Teisset,¹ Robert Bessing,¹ Knut Michel,¹ Reinhard Kienberger,^{2,3} and Thomas Metzger¹

¹TRUMPF Scientific Lasers GmbH + Co. KG, Feringastr. 10a, 85774 Unterföhring-München, Germany

²Department of Physics, Technische Universität München, James-Frank-Str., 85748 Garching, Germany

³Max-Planck-Institut für Quantenoptik, Hans-Kopfermann-Str. 1, 85748 Garching, Germany

*Stephan.Prinz@de.TRUMPF.com

Abstract: Short-pulse-pumped optical parametric chirped pulse amplification (OPCPA) requires a precise temporal overlap of the interacting pulses in the nonlinear crystal to achieve stable performance. We present active synchronization of the ps-pump pulses and the broadband seed pulses used in an OPCPA system with a residual timing jitter below 2 fs. This unprecedented stability was achieved utilizing optical parametric amplification to generate the error signal, requiring less than 4 pJ of seed- and 10 μ J of pump-pulse-energy in the optical setup. The synchronization system shows excellent long-term performance and can be easily implemented in almost any OPCPA system.

©2014 Optical Society of America

OCIS codes: (140.3425) Laser stabilization; (140.7090) Ultrafast lasers; (190.4970) Parametric oscillators and amplifiers.

References and links

1. A. Vaupel, N. Bodnar, B. Webb, L. Shah, and M. Richardson, "Concepts, performance review, and prospects of table-top, few-cycle optical parametric chirped-pulse amplification," *Opt. Eng.* **53**(5), 051507 (2014).
2. A. Dubietis, R. Butkus, and A. P. Piskarskas, "Trends in chirped pulse optical parametric amplification," *IEEE J. Sel. Top. Quantum Electron.* **12**(2), 163–172 (2006).
3. H. Fattahi, H. G. Barros, M. Gorjan, T. Nubbemeyer, B. Alsaif, C. Y. Teisset, M. Schultze, S. Prinz, M. Häfner, M. Ueffing, A. Alismail, L. Vámos, A. Schwarz, O. Pronin, J. Brons, X. T. Geng, G. Arisholm, M. Ciappina, V. S. Yakovlev, D.-E. Kim, A. M. Azzeer, N. Karpowicz, D. Sutter, Z. Major, T. Metzger, and F. Krausz, "Third-generation femtosecond technology," *Optica* **1**(1), 45 (2014).
4. C. Teisset, M. Schultze, R. Bessing, M. Häfner, S. Prinz, D. Sutter, and T. Metzger, "300 W Picosecond Thin-Disk Regenerative Amplifier at 10 kHz Repetition Rate," in *Advanced Solid-State Lasers Congress Postdeadline* (Optical Society of America, 2013), pp. JTh5A.1.
5. T. Metzger, A. Schwarz, C. Y. Teisset, D. Sutter, A. Killi, R. Kienberger, and F. Krausz, "High-repetition-rate picosecond pump laser based on a Yb:YAG disk amplifier for optical parametric amplification," *Opt. Lett.* **34**(14), 2123–2125 (2009).
6. M. Schulz, R. Riedel, A. Willner, T. Mans, C. Schnitzler, P. Russbuehlt, J. Dolkemeyer, E. Seise, T. Gottschall, S. Hädrich, S. Duesterer, H. Schlarb, J. Feldhaus, J. Limpert, B. Faatz, A. Tünnermann, J. Rossbach, M. Drescher, and F. Tavella, "Yb:YAG Innoslab amplifier: efficient high repetition rate subpicosecond pumping system for optical parametric chirped pulse amplification," *Opt. Lett.* **36**(13), 2456–2458 (2011).
7. K.-H. Hong, A. Siddiqui, J. Moses, J. Gopinath, J. Hybl, F. Ö. Ilday, T. Y. Fan, and F. X. Kärtner, "Generation of 287 W, 5.5 ps pulses at 78 MHz repetition rate from a cryogenically cooled Yb:YAG amplifier seeded by a fiber chirped-pulse amplification system," *Opt. Lett.* **33**(21), 2473–2475 (2008).
8. T. Eidam, S. Hanf, E. Seise, T. V. Andersen, T. Gabler, C. Wirth, T. Schreiber, J. Limpert, and A. Tünnermann, "Femtosecond fiber CPA system emitting 830 W average output power," *Opt. Lett.* **35**(2), 94–96 (2010).
9. J. Rothhardt, S. Demmler, S. Hädrich, J. Limpert, and A. Tünnermann, "Octave-spanning OPCPA system delivering CEP-stable few-cycle pulses and 22 W of average power at 1 MHz repetition rate," *Opt. Express* **20**(10), 10870–10878 (2012).
10. B. C. Stuart, M. D. Feit, S. Herman, A. M. Rubenchik, B. W. Shore, and M. D. Perry, "Nanosecond-to-femtosecond laser-induced breakdown in dielectrics," *Phys. Rev. B Condens. Matter* **53**(4), 1749–1761 (1996).
11. S. Witte and K. S. E. Eikema, "Ultrafast Optical Parametric Chirped-Pulse Amplification," *IEEE J. Sel. Top. Quantum Electron.* **18**(1), 296–307 (2012).
12. S. Hädrich, J. Rothhardt, M. Krebs, S. Demmler, J. Limpert, and A. Tünnermann, "Improving carrier-envelope phase stability in optical parametric chirped-pulse amplifiers by control of timing jitter," *Opt. Lett.* **37**(23), 4910–4912 (2012).

13. N. Ishii, C. Y. Teisset, T. Fuji, S. Kohler, K. Schmid, L. Veisz, A. Baltuska, and F. Krausz, "Seeding of an eleven femtosecond optical parametric chirped pulse amplifier and its Nd^{3+} picosecond pump laser from a single broadband Ti:Sapphire oscillator," *IEEE J. Sel. Top. Quantum Electron.* **12**(2), 173–180 (2006).
14. S. Klingebiel, I. Ahmad, C. Wandt, C. Skrobol, S. A. Trushin, Z. Major, F. Krausz, and S. Karsch, "Experimental and theoretical investigation of timing jitter inside a stretcher-compressor setup," *Opt. Express* **20**(4), 3443–3455 (2012).
15. A. Schwarz, M. Ueffing, Y. Deng, X. Gu, H. Fattahi, T. Metzger, M. Ossiander, F. Krausz, and R. Kienberger, "Active stabilization for optically synchronized optical parametric chirped pulse amplification," *Opt. Express* **20**(5), 5557–5565 (2012).
16. C. Manzoni, S.-W. Huang, G. Cirmi, P. Farinello, J. Moses, F. X. Kärtner, and G. Cerullo, "Coherent synthesis of ultra-broadband optical parametric amplifiers," *Opt. Lett.* **37**(11), 1880–1882 (2012).
17. D. H. Sutter, D. Bauer, J. Kleinbauer, A. Budnicki, M. Wolf, C. Tan, R. Gebs, P. Wagenblast, and S. Weiler, "Ultrafast Disk Lasers and Amplifiers," in *Lasers, Sources, and Related Photonic Devices* (Optical Society of America, 2012), pp. AM2A.1.
18. M. Schultze, S. Prinz, C. Y. Teisset, M. Haefner, R. Bessing, K. Michel and T. Metzger, „CEP-Stable, Few-Cycle OPCPA System with more than 15 W of Average Output Power at 300 kHz,” presented at 6th EPS-QEOD EUROPHOTON CONFERENCE, Neuchatel, Switzerland, 24–29 Aug. 2014, paper ThE-T1-O-03.

1. Introduction

OPCPA is nowadays commonly used as a powerful technique to generate few-cycle ultrashort laser pulses with high energies and high peak intensities [1–3]. In contrast to classical laser amplification schemes based on stimulated emission, no energy is stored inside the gain medium of an optical parametric amplifier (OPA), i.e. a nonlinear crystal. This results in low thermal effects and an enhanced contrast ratio. High parametric gain of up to 10^6 can be routinely achieved within an extremely broad amplification bandwidth and with an excellent output beam quality [2].

With a variety of different powerful pump sources available today [3–9], short pump pulse durations close to 1 ps turned out to be favorable in the amplification process [3] because of an increased damage threshold in the nonlinear crystals [10]. This allows for higher pump intensities and therefore shorter crystals, supporting a broader amplification bandwidth while maintaining a high gain and a simplified dispersion management. On the other hand, due to the quasi instantaneous nature of the parametric process itself, ps-pump pulses accentuate the demands on the pulse timing. In a ps-pumped OPCPA, a timing jitter in the order of some hundred femtoseconds already leads to an insufficient pulse overlap, resulting in intolerable spectral shifts, instable pulse energies, varying pulse durations, carrier-envelope phase instabilities and reduced efficiencies [11, 12].

A first step to synchronize pump and seed pulses is passive optical synchronization, where a single master oscillator seeds both the pump and OPA [13]. This ensures that temporal drifts in the master oscillator equally affect the pump and seed pulses. However, thermal drift, air turbulences and vibrations in the optical setup [14, 15] lead to a temporal mismatch in the seed and pump pulse arrival times. Therefore an active compensation of the remaining relative timing jitter is mandatory to achieve long-term stable OPCPA performance, even in optically synchronized OPCPA systems.

An appropriate closed loop compensation scheme comprises a delay element that allows for the compensation of the relative timing jitter by adjusting the optical path length, delay sensitive detection and control electronics. The measurement on fs-timescale is challenging, because a direct measurement with conventional electronics, e.g. photodiodes, is not possible due to their limited response time. By utilizing nonlinear processes which strongly depend on the relative timing between the involved pulses, this problem can be circumvented. Following this general scheme, an active synchronization system based on frequency resolved cross correlation has been successfully implemented with a residual relative RMS timing jitter of $\sigma = 24$ fs [15]. In this approach, the error signal was generated by sum frequency generation (SFG), requiring relatively large pulse energies to achieve a sufficiently strong signal for detection.

A synchronization system based on a balanced optical cross-correlator (BOC) with a residual timing jitter below 30 as was presented in [16] as a basis for coherent pulse synthesis. Such a high resolution comes at the cost of a small measurement range, thus being solely

applicable for an inherently small timing jitter in the range of a few fs. This is typically not the case for high power OPCPA systems with large path length differences between pump and seed pulses [15]. Additionally, the BOC scheme comes with a comparably complex optical and electronic setup.

Here we present an active synchronization system which synchronizes the pump and seed pulses in time with less than 2 fs remaining timing jitter in a frequency band up to 1 kHz. The performance of the stabilization system in [15] is thus improved by one order of magnitude. The major difference is the use of parametric amplification as nonlinear process in combination with an in-house developed detector for the measurement of the pulse timing jitter. With this approach, a few pJ of seed pulse energy are already sufficient in the optical setup, making the system easily implementable in almost any OPCPA setup without sacrificing much seed energy for the main amplifier.

2. Experimental implementation

The setup of our system is shown schematically in Fig. 1. An octave spanning Ti:Sapphire oscillator (Venteon Pulse:One OPCPA) serves as a broadband seed source, delivering pulses with a duration of 6 fs and a pulse energy of 2.5 nJ at a repetition rate of 75 MHz, centered around 800 nm. A Yb:YAG thin-disk regenerative amplifier based on a modified TRUMPF TruMicro 5000 [17] is used as a pump source and is seeded directly by the second output of the Ti:Sa oscillator at $\lambda = 1030$ nm, providing optical synchronization between both systems. At a repetition rate of 300 kHz, the regenerative amplifier delivers up to 200 W of average output power with a pulse duration of 1.3 ps. The pulses are frequency doubled in a 1.5 mm LBO crystal, yielding up to 140 W ($E_p = 467 \mu\text{J}$) with a pulse duration of 1.2 ps at $\lambda = 515$ nm. The high SHG conversion efficiency of 70% is reached because of the excellent temporal and spatial beam profile of the regenerative amplifier.

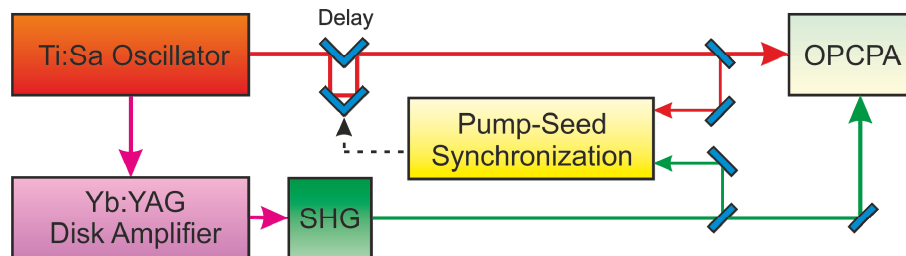


Fig. 1. Schematic setup of our system: Pump and seed pulses are directly derived from a broadband Ti:Sapphire oscillator. The pump pulses at $\lambda = 1030$ nm are amplified in a Yb:YAG regenerative thin disk amplifier and frequency doubled in a SHG-stage. The pump-seed synchronization system is implemented close to the OPCPA and controls an adjustable delay stage.

The optical part of the pump seed synchronization is located close to the OPCPA in order to avoid additional timing jitter accumulation after the detection. In our system, a fixed amount of 20% of the seed energy and 2% of the pump energy, corresponding to $E_s = 0.5$ nJ and $E_p = 10 \mu\text{J}$, are split off before the OPCPA and used to generate the error signal. The detected signal is fed into a proportional-integral controller driving a delay stage, compensating the timing jitter by adjustment of the optical path length in the seed arm.

2.1 Optical setup

A detailed overview of the optical setup of our system is given in Fig. 2. After a 80:20-beamsplitter, the transmitted broadband seed pulses are stretched in time by a 100 mm SF57 bulk glass block to a duration of ~ 12 ps FWHM. Seed and pump beam are focused into a 5 mm BBO crystal, cut at $\theta = 24^\circ$, under a noncollinear angle of $\alpha = 2.3^\circ$ to achieve broadband phase matching. The focal spot size of the seed beam ($\omega_s \approx 100 \mu\text{m}$) has been chosen to be

slightly larger than the pump ($\omega_p \approx 70 \text{ } \mu\text{m}$) to ensure a good overlap inside the crystal and to reduce the influence of beam pointing on the signal intensity.

According to the relative delay between the stretched seed pulse and the short pump pulse, a different spectral fraction of the seed spectrum is amplified in the OPA. The inset in Fig. 2 shows the simulated output of the OPA at different group delays (GD). An increasing delay leads to a spectral shift of the central wavelength in the amplified signal, which is only dependant on the dispersion of the seed.

The simplest way to measure this signal would be using a spectrometer. However, the long integration time of most spectroscopic devices, usually in the ms-range, limits the acquisition bandwidth, making the detection of fast jitter contributions impossible. Therefore, a blazed transmission grating with 300 lines/mm is used to diffract the signal at a wavelength dependent angle through a projection lens ($f = 50 \text{ mm}$) onto a position sensitive detector (PSD), where the position of the centroid is detected. With this combination of grating, lens and a PSD size of 5 mm, we are able to measure a relative timing delay of up to $\pm 10 \text{ ps}$. Thanks to the wide detection range the system is intrinsically stable even in case of strong transient events.

The detected position is directly correlated to the relative timing delay between the two pulses and thus serves as error signal for the control loop. The delay stage combines a piezo actuator with a travel range of $100 \text{ } \mu\text{m}$ (Piezosystem Jena) and a linear translation stage (Physik Instrumente) to compensate for fast and slow temporal drifts, respectively. A prism retroreflector with a total mass of 11 g is mounted on top of the piezo stage. The low mass does not reduce its nominal resonance frequency of 790 Hz significantly.

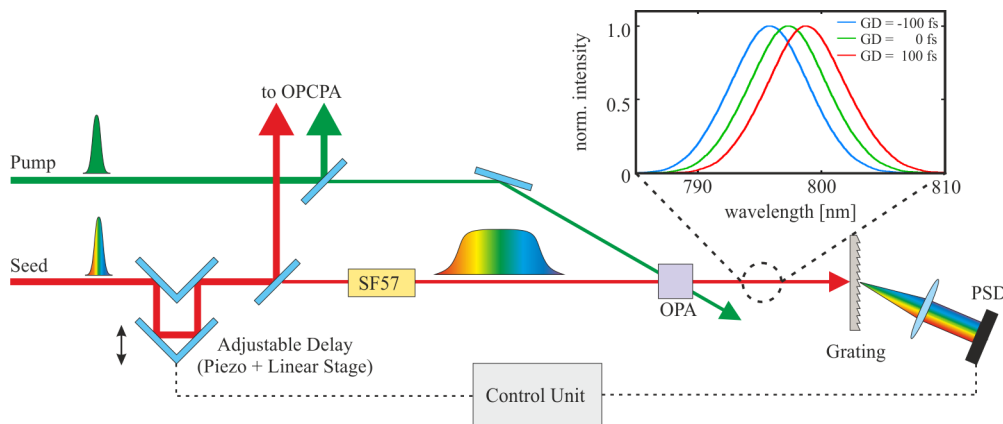


Fig. 2. Optical setup to detect the timing jitter between pump and seed pulses. SF57, bulk glass block; OPA, optical parametric amplifier; PSD, position sensitive detector. The inset shows the simulated output of the OPA at different relative group delays (GD).

In order to characterize the residual timing jitter, calibration of the system around the setpoint was performed prior to the measurement. The calibration curve around the center of the PSD is obtained by stepwise introducing an artificial timing delay to the system via the linear translation stage and measurement of the corresponding centroid position shift. A linear regression finally yields the calibration factor.

A seed pulse energy of 500 pJ was used in the setup because of the fixed ratio of the employed broadband beamsplitter. To determine the minimum possible seed pulse energy, a variable neutral density filter was inserted at the input of the optical setup. A value as low as $E_s = 4 \text{ pJ}$ could be used without any degradation of the system's performance, leaving even more energy available for the use in the following OPCPA.

2.2 Electronics

The key to a high performance of the synchronization is not only the generation of the optical error signal, but also its detection and compensation. Compared to SFG, where the generated

error signal is spatially separated from the pump and seed pulses, the OPA signal at 300 kHz is overlapped by the unamplified 75-MHz seed pulses. If not properly treated, this will generate a noisy offset inside the PSD readout electronics which decreases the signal to noise ratio (SNR) and limits the accuracy of the measurement. To deal with this issue, we use an in-house development for the detection of the signal's centroid. In our analog readout, the offset is detected and subtracted from the acquired PSD signal. This yields a clean detected pulse with high position fidelity. After a sample & hold circuit, the detected value is converted into a digital signal and sent to the control unit.

Our detection system was characterized over the whole detection area at a pulse energy of 500 pJ. The SNR was measured to be as high as 80 dB in the center and 70 dB in the outer regions of the PSD. At 60% lower pulse energies (200 pJ), the SNR is slightly decreased by ~6 dB. The positional error related to the decreased pulse energy in the center (outside) of the PSD is below 0.1% (0.7%), making the system immune to intensity noise. The maximum data acquisition rate of our PSD electronics is currently 500 kHz, permitting measurements on a single shot basis.

3. Synchronization results

3.1 Free-running long-term drift

The relative long-term drift between pump and seed pulses in our system has been evaluated at full output power of the pump source in Fig. 3 without synchronization. Detection was done with a spectrometer (Ocean Optics HR4000, 3 ms integration time, one spectrum every 20 s) directly after the OPA output. The change in the peak wavelength of the output spectrum was recorded and translated to the relative timing delay between pump and seed pulses using the group delay dispersion (GDD) of the inserted SF57 glass block at 800 nm. We measured a total drift of more than 4 ps over two hours, which means a complete temporal separation of pump and seed pulses and underlines the need for an active synchronization system.

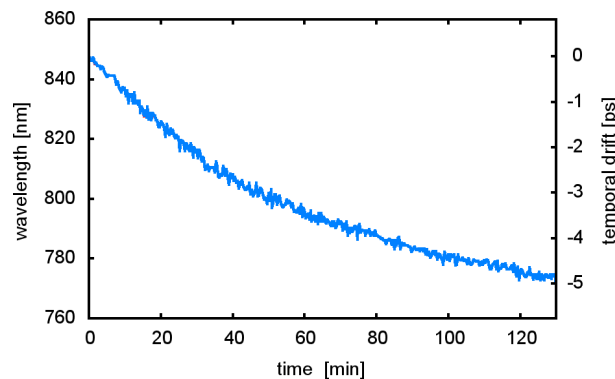


Fig. 3. Relative long-term drift between pump and seed pulses at full output power of the regenerative disk amplifier, measured with a spectrometer.

3.2 Short-term drift

The short-term timing jitter of the system was measured using the PSD with an acquisition bandwidth of 1 kHz, well above the piezo resonance frequency. We expect no significant timing jitter contribution at higher frequencies in our system. The applied low-pass filter increases the SNR of our detection electronics to 103 dB, corresponding to a resolution limit of only 140 as.

The regenerative amplifier was running at full output power, where thermal effects are most pronounced. Figure 4(a) shows the relative timing delay between pump and seed pulses in the free-running case and with active synchronization, measured in-loop over 10 s. We observed a change in timing delay of up to 200 fs in the first 5 seconds of the measurement, which is already more than 15% of the pump pulse duration and not tolerable for an OPCPA.

The situation is improved significantly in the case of active synchronization. The pulse arrival times are locked relative to each other with a residual timing jitter of $\sigma < 2$ fs, corresponding to less than 0.2% of the pump pulse duration.

The reliability of the system and its long-term performance are shown in Fig. 4(b). The data is recorded over two hours at an acquisition rate of 10 Hz. The feedback signal is enabled after 2 min (Inset, Fig. 4(b)), instantly locking the timing delay and cancelling out all the long-term drifts of the system. With the currently employed delay stage, we are able to compensate for a total drift of 667 ps, potentially enabling days of stable synchronization.

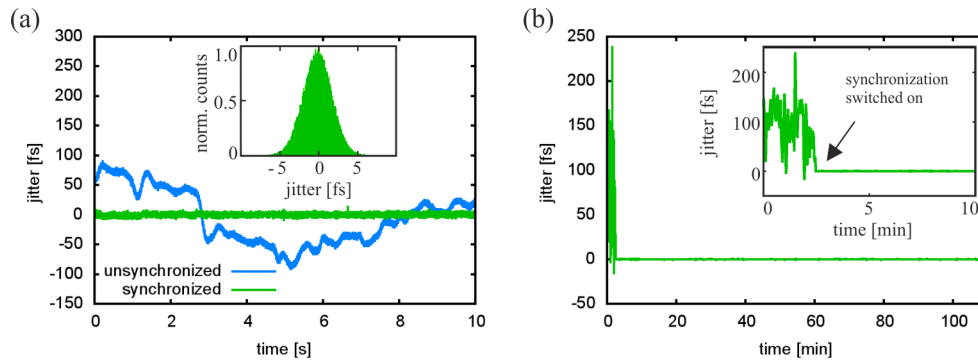


Fig. 4. (a) Short-term timing jitter unsynchronized (blue) and with active synchronization (green). The RMS timing jitter in the stabilized case is reduced to $\sigma < 2$ fs. The inset shows a histogram of the measured timing jitter values. (b) Long-term measurement of the timing delay between the pump and seed pulses. Inset: Activation of the stabilization after 2 min.

3.3 Spectral analysis

Figure 5 shows the amplitude spectrum of the acquired data in case of the free-running system and with active synchronization, obtained by Fourier transformation. The main distribution to the timing jitter is located in a bandwidth below 10 Hz, which can be compensated by the synchronization system.

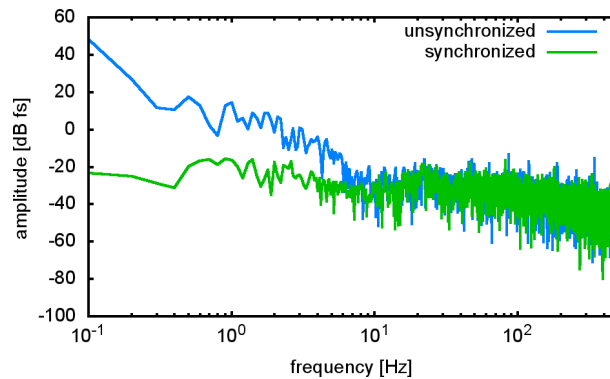


Fig. 5. Amplitude spectrum of pulse timing jitter without synchronization (blue) and with active synchronization (green).

From this analysis, the bandwidth of the closed loop feedback is estimated to be larger than 10 Hz. Although this performance is absolutely sufficient for our setup, the bandwidth could be further increased by using a faster piezo actuator with an increased resonance frequency in the kHz-regime.

4. Conclusion and outlook

We presented an active synchronization system which reduces the relative timing jitter between pump and seed pulses in an OPCPA below $\sigma = 2$ fs in a frequency band up to 1 kHz. The system currently supports a measurement range of up to 20 ps and thus represents the highest dynamic range which has been demonstrated in a pulse synchronization system so far.

An in-house developed detection system based on a PSD with an exceptional SNR of up to 80 dB allows the precise measurement of the relative pulse timing delay. Because OPA is utilized in the detection scheme, less than 4 pJ of seed and 10 μ J of pump pulse energy are needed for the generation of the optical error signal. Lower pump pulse energies are theoretically feasible if the pump intensity inside the OPA is kept constant. Therefore, an implementation in almost any OPCPA setup is possible without significantly sacrificing energy for the main amplifier, which has been a drawback of earlier systems. With an excellent long-term performance, the system is able to compensate for thermal drifts in the range of many ps, enabling a stable OPCPA performance over days. The system is currently deployed in a 300-kHz multistage OPCPA laser system, delivering CEP-stable sub-7-fs pulses with more than 15 W of average output power [18].

To circumvent the need for electronic background rejection of the unamplified seed pulses in the detector, the usage of the generated idler as error signal is an attractive option. At present, the lack of suitable PSDs with a detection range in the NIR hinders this approach.

Since the achievable remaining timing jitter is limited by the noise floor of the detection electronics, even further improvement of the system's performance might be possible in the future.